CIGRE SESSION 48

Paris 2020

A3-204

In-service Diagnosis of Grading Capacitor Dielectric Deterioration

P MOORE[1] and K WILLIAMS
Elimpus Ltd and National Grid
United Kingdom

SUMMARY

Disruptive dielectric failure of circuit breaker grading capacitors is well known in AIS and GIS transmission switchgear. This paper describes a methodology, initially developed to investigate the cause of damage to interrupter nozzles during reactor CB opening operations, that has proved suitable for grading capacitor Partial Discharge (PD) measurement. A key technology used in the investigation is radiometric PD location which allows identification of the origin of individual PD events from a CB via the reception of RF impulses. During the arcing period of a CB operation, impulses are emitted from the interrupters as the contacts move. However, field tests under CB open operations revealed additional PD impulses were also recorded immediately after the extinction of the current when the grading capacitors were highly stressed. This effect was repeatable over many operations until the defective grading capacitor was replaced. The defect in the grading capacitor was confirmed by testing in a HV laboratory which revealed abnormal results in both Tanδ and IEC60270 PD tests. As a consequence the capacitor was stripped down revealing extensive damage to many of the individual capacitor units within the assembly, confirming that the capacitor was effectively at its end of life. Analysis of the PD data recorded during the investigation demonstrated that the duration and intensity of the PD increased over a period of 78 days involving 14 separate CB open operation measurements. One particular PD metric, based on assessing the number of emitted PD impulses that exceeded an amplitude of 0.1V, indicates that the remaining life of this capacitor to be ~25 operations after the amplitude threshold was exceeded. A significant benefit of this measurement approach is that the CB remains in service during testing.

KEYWORDS

High Voltage, Circuit Breaker, Switching, Overvoltage, Grading Capacitor, Partial discharge, Radio Frequency, Diagnostic.

[1] phil.moore@elimpus.com

1. INTRODUCTION

Disruptive dielectric failure of grading capacitors has been widely reported in both GIS [1] and AIS [2] transmission switchgear. These events can cause extensive damage to the circuit breaker (CB) and, in some cases, to neighbouring HV equipment. The occurrence of failure has been linked to switching duty which places reactive switchgear, operating typically once a day, at particular risk.

This paper describes a method for determining the presence of partial discharge (PD) on grading capacitors during service operations, and the experience of application on an AIS 420kV reactive circuit breaker. The development of this method was an outcome from a study into the switching behaviour of reactor circuit breakers following several failures and near-misses (i.e. removed from service before failure) of 420 kV, hydraulically operated gas circuit breaker interrupters when switching reactor loads. In one specific example, extensive damage to the outer phase interrupter nozzles was discovered despite the CB being fitted with a controlled switching device (i.e. relay to avoid arc re-ignitions), bringing into question the correct operation of the latter. The investigation was subsequently conducted to determine the correct operation of CB during reactor open operations focussing particularly on the operation of the interrupters and the controlled switching device. The methodology used for this investigation was able to report on both these points but, additionally, detected a failing grading capacitor enabling its removal from service - without incident - at its effective end of life point.

A key technology used in this investigation is the radio frequency (RF) detection of partial discharge (PD) emissions. In air insulated substations (AIS) the occurrence of PD within HV equipment causes the radiation of short duration RF impulses, typically ~1µs in duration, which can be detected over distances of up to 50 m using wideband receiving antennas. RF impulse emission is due to the fast rise-time of current pulses associated with PD and is heavily influenced by metallic components adjacent to the location of the insulation defect – e.g. busbars, earth straps – which act as PD transmitting antennas. Due to the typical sizes of the latter in transmission substations, the radiation of PD impulses is normally restricted to a RF range below 1 GHz. The significant benefit of RF PD measurement is that the HV equipment can remain in-service since no physical or electrical connection is required in its deployment. Additionally, by timing the arrival of the PD impulses to sub-nanosecond accuracy across an array of PD receiving antennas of known positions, the location of the PD source can be calculated in relation to the substation equipment. PD locating systems based on this principle are referred to as 'radiometric' PD location systems [3] and have been applied to AIS substation applications [4]. Additionally, radiometric systems have been applied to CB timing measurement [5,6] since CB operations similarly generate short duration RF impulse emissions.

2. METHODOLOGY

2.1 Field measurements

The investigation was performed on 400kV gas CB connected to a 200 MVAr reactor. A summary of the monitored values recorded during each open operation of the CB is shown in Table 1 below.

Measurement	Sensor	Sampling frequency
Interrupter/grading capacitor PD emissions	Antenna (x4)	2.5 GSps
CB trip coils current	Electronic current clamp (x3)	20 kSps
Reactor terminal voltage	Electric-field sensor (x3)	20 kSps

Table 1 Field measurements made during CB open tests

Each measurement was made with a separate recording unit; all units were synchronised. Both PD and electric field sensor measurements required further processing as described in the following sections.

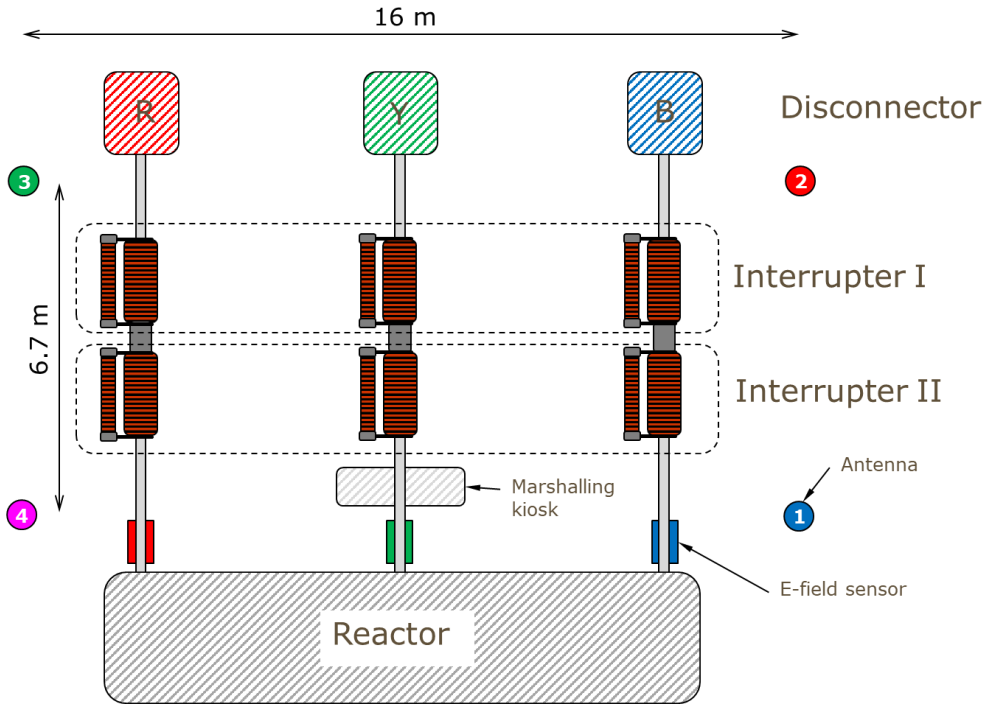

Figure 1 Plan view showing field measurement arrangements (not to scale)

Figure 1 shows a plan view of the antennas and electric-field sensors which were connected, via coaxial cable, to recording units housed within a vehicle situated close to the reactor. Similar connections were made to the trip coil current clamps that were applied to wiring within the marshalling kiosk. To make a recording, the CB open operation was requested, via mobile phone, directly to the control room; the recording equipment was armed immediately before the remote trip command was issued to ensure that the recording buffers were sufficient to capture data up to 1 second after the reactor was disconnected.

2.2 PD location

RF impulses may be emitted from the CB due to both PD – i.e. unwanted discharges across highly stressed dielectric regions – and from the current interruption process of the CB. In this paper any RF impulsive emissions from the CB will be referred to as 'PD' irrespective of the mode of generation.

PD impulses were captured using the array of four antennas shown in Figure 1 and high-speed digital recording equipment operating at 2.5 GSps. A PD impulse, moving at the speed of light through air, will travel 120 mm between samples. The antennas had a flat frequency response in the region 10-1000 MHz [3] and were connected using coaxial cables of identical propagation delay. The interrupter origin of a PD impulse is found by comparing ideal and measured time delays from the four antennas. The ideal time delays are calculated using laser-based site measurements taken from the antenna to the mid-point of each interrupter. For example, the distances between red interrupter I and each of the antennas 1-4 are 16.6 m, 15.9 m, 9.6 m and 10.7 m respectively. Taking the nearest antenna (3) as the reference and converting the path length differences into time delays (where 0.3 m ≡ 1 ns) gives +21 ns, +23 ns, 0 and +4 ns respectively. Typical PD impulses recorded during the open operation of the same interrupter are shown in Figure 2 – note that the colours of the antennas in Figure 1 relate to the waveforms shown in Figures 2 and 3. The upper graph shows the four impulses in their entirety which are ~0.2 µs in length; the majority of the energy in the

impulses lies below 100 MHz. The lower graph shows the detail around the start of the impulses where the signal arrives at antenna 3 (green) shortly before antenna 4 (magenta), whereas the signals at antennas 1 (blue) and 2 (red) can be seen to be ~20 ns later. The time delays evident in Figure 2 are approximately as the previous calculation, although in practice a leeway of ±3 ns between the calculated and measured time delays can be tolerated without affecting the result since the calculations assume that the impulse is radiated from the mid-point of the interrupter which is not necessarily the case. An example for the red phase II interrupter open operation is shown in Figure 3 from which it is apparent that the impulse arrives at antenna 4 (magenta) before antenna 3 (green). Thus the measurements can differentiate between emissions from both red phase interrupters. Similar calculations can be applied to determine the origin of interrupters on the yellow and blue phases. Note that this process will also identify the grading capacitors as origins during the period that the interrupters are open. PD arising from other areas of the substation, if present during the measurements, will have differing time delays to the above and can be discarded.

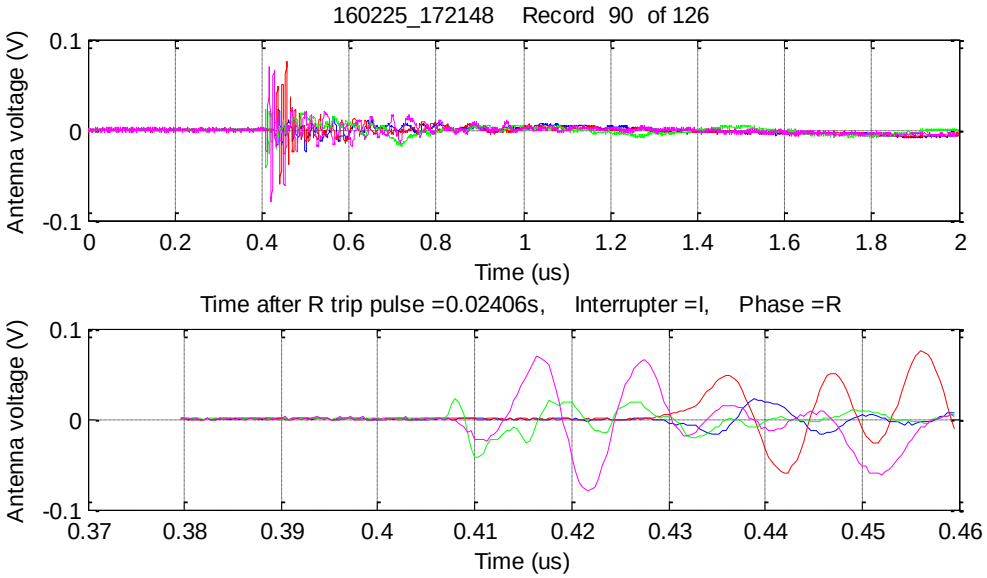

Figure 2 Antenna signals recorded for red phase interrupter I emission.

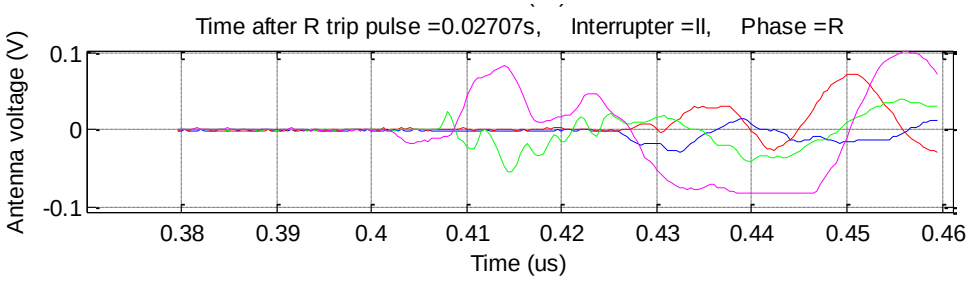

Figure 3 Antenna signals recorded for red phase interrupter II emission.

2.3 Reactor terminal voltage calculation

The reactor terminal voltages could not be directly measured during an open operation since there was no voltage transformer (VT) between the CB and the reactor. To overcome this issue three electric-field sensors (which provide outputs that are capacitively coupled to the overhead reactor terminals) were deployed between the CB and the reactor as shown in Figure 1. A brief description of the construction of the sensors is given in Appendix 1. The sensors were housed in plastic boxes and positioned on the ground directly beneath the busbars, see Figure 1. Consequently, each sensor will sense the combination of all three phase voltages in varying proportions dependent on the distance to the conductors. In order to derive the busbar voltages it is necessary to decouple the electric field

sensors outputs. The relationship between the p.u. busbar voltages, v_r, v_y, v_b, and the electric field sensors outputs, s_r, s_y, s_b, is given in the matrix equation below. The constants in the 3x3 matrix were found iteratively by comparing the sensor outputs (with the CB closed) with busbar VT outputs.

$$\begin{bmatrix} v_r \\ v_y \\ v_b \end{bmatrix} = \begin{bmatrix} 9.55 & -4.86 & 1.01 \\ -4.84 & 13.14 & -4.65 \\ 0.90 & -4.38 & 9.47 \end{bmatrix} \begin{bmatrix} s_r \\ s_y \\ s_b \end{bmatrix}$$

This process is illustrated in Figures 4 and 5 below which show the electric field sensor outputs and the derived busbar phase voltages respectively at the point of current interruption. Note that there is a 'beating' effect evident in the reactor transients on all phases. This is due to the transient frequency being slightly different on each phase.

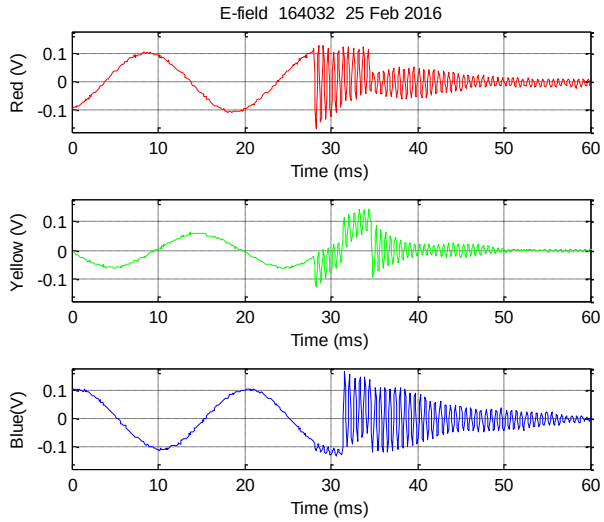

Figure 4 E-field sensor outputs from reactor terminal voltage measurements

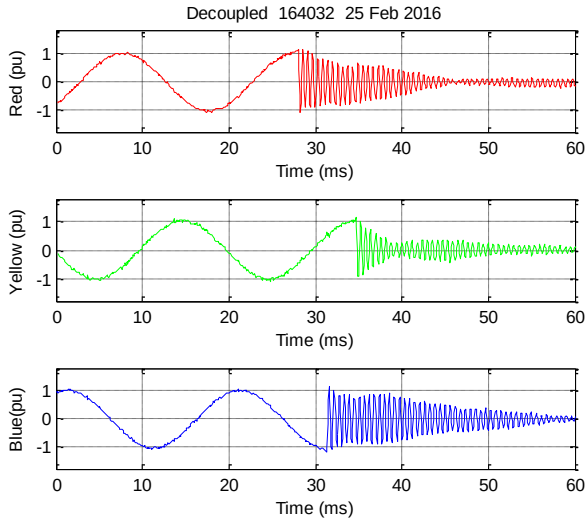

Figure 5 Reactor terminal voltages calculated from E-field sensor outputs

3. RESULTS

3.1 After grading capacitor replacement

Although counter-intuitive, it is instructive to begin with results taken at the end of the investigation which present the operation of an 'ideal' CB, since by this point both the interrupters and grading capacitors had been replaced. Figure 6 shows the PD emissions in relation to the trip coil pulse and reactor terminal voltages for the red phase. The PD impulses are identified to the relevant interrupter and displayed as discrete values at the time of emission where the height of the bar corresponds to the peak of the impulse waveform. The disconnection of the reactor at ~28 ms coincides with the change of the reactor terminal voltage from 50 Hz to a decaying transient oscillation of 1709 Hz, the latter being caused by the magnetic energy stored in the core interacting with stray capacitances, including the bushing and winding capacitances. It can be seen that each interrupter emits a short series of RF impulses that begin at approximately 7ms before disconnection and continues until current extinction. It is speculated that the first impulse emission is due to the transition, within the interrupter, between the arcing contacts opening and the start of the arc. Instabilities in the arc, or possibly movement of the contacts, cause more emissions until the arc extinguishes. Note, for an 'ideal' breaker, there are only emissions during the arcing period. The number of impulses emitted from the interrupters during the arcing period increases with length of operational service, this is discussed further in Appendix 2.

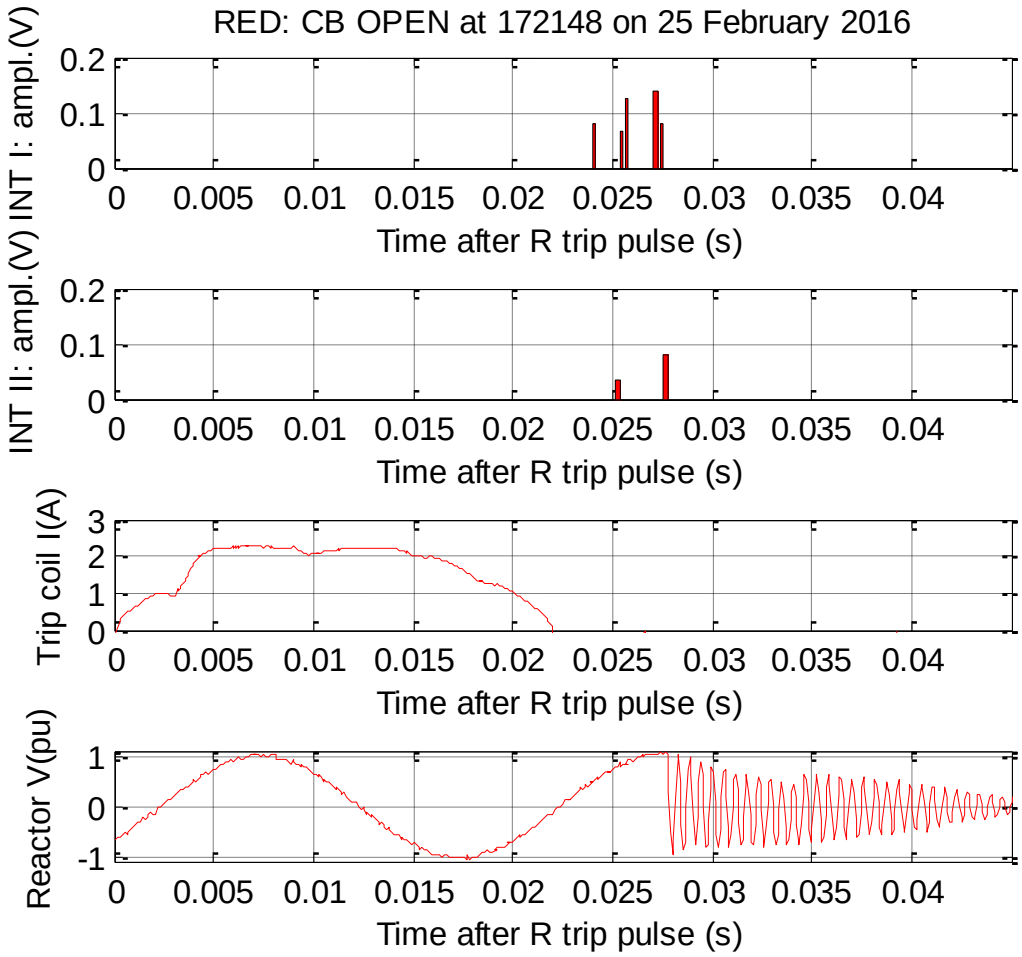

Figure 6 Open operation for 'ideal' breaker

Results for the blue and yellow phases are essentially very similar excepting that the start of the trip pulse and the reactor disconnection occur 3.3 ms and 6.6 ms respectively later than the red phase. For reference, the figures are given in Appendix 3.

3.2 Before grading capacitor replacement

At the time of the first investigation into the CB in November 2015, recorded data demonstrated that the impulse emission was extended beyond the arcing period into the reactor transient voltage period on interrupter I on the red phase – all other interrupters were unaffected - a typical example is shown in Figure 7.

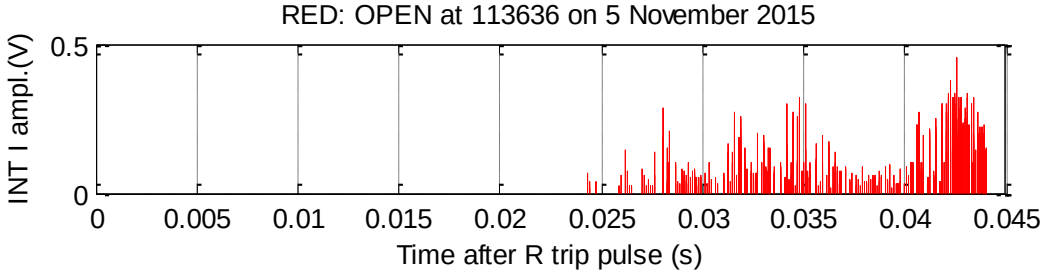

Figure 7 Open operation including grading capacitor PD from interrupter I.

For brevity only the impulse emission plot for interrupter I is shown in Figure 7, however the trip coil current and the reactor terminal voltage – and therefore the reactor disconnection - appear

identically as in Figure 6. It is apparent from Figure 7 that significant PD impulses are emitted from interrupter I for ~16 ms following the reactor disconnection. The operation was repeated 6 further times with similar results.

Initially it was suspected that the interrupters were at fault and these, but not the grading capacitors, were duly changed in January 2016. Following the refit, the tests described above were repeated (8 open operations in total) and yielded similar results to Figure 3: significant PD emission being detected from interrupter I. At this point it was concluded that the grading capacitor was the cause of the PD. Consequently, in February 2016, the grading capacitors on the red and yellow phases were replaced. Again, the tests were repeated and yielded the results of Figure 6 consistently (4 open operations in total) which were regarded as representing the 'ideal' open operation of the CB.

3.3 Grading capacitor investigation

The grading capacitors removed from the CB were further investigated in a HV laboratory. Initial tests using both Tanδ and IEC60270 PD tests yielded the results of Table 2.

Phase	Interrupter	% dissipation factor	PD inception voltage
Red	I	0.31	9 kV
Red	II	0.025	51 kV
Yellow	I	0.025	51 kV
Yellow	II	0.032	37 kV

Table 2 Results of HV laboratory testing on grading capacitors removed from CB

It is apparent that the HV laboratory tests independently identify the red phase interrupter I grading capacitor as being defective, similarly to the field tests. With the diagnosis confirmed by two independent methods, the defective grading capacitor was stripped down to investigate the source of the dielectric failure. The defective grading capacitor, manufactured in 2002, was an oil-filled, 2000 pF, 145 kV device, rated at 420 kV for 72 seconds and containing 256 individual capacitor units. Disassembly revealed that ~30% of the capacitor units were damaged – a typical foil from a damaged capacitor unit is shown in Figure 8, where it will be apparent that significant erosion of the foil has occurred due to sparking caused by overvoltage during the reactor transient period of the CB open operation. It is unlikely that the capacitor would have withstood further CB open operations and it is therefore concluded that the capacitor was, for all practical purposes, at its end of life when removed from service.

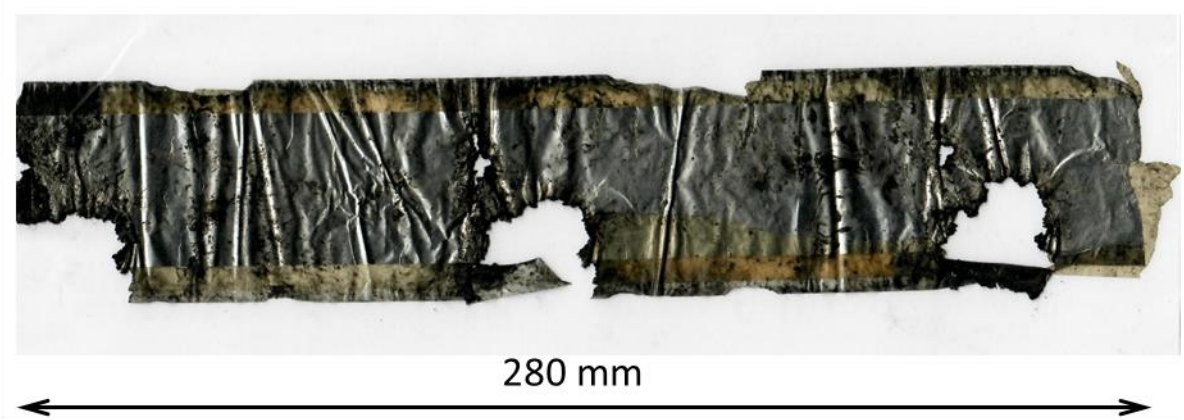

Figure 8 Damage to the foil of an individual capacitor unit.

4. USE OF TESTING METHOD AS A PROGNOSTIC TOOL

Testing on the CB began in November 2015 and continued in January 2016: on both occasions the PD from the grading capacitor was detected. The results were recorded at the start and end of a time scale spanning 78 days, during which the CB remained in service (there are 10 operations during this period that were not recorded). It is therefore possible, assuming that the grading capacitor was end of life after the January tests, to analyse the recorded data to establish if any evident change in the PD emissions occurred which can act as a predictor for the remaining life of the grading capacitor. Figure 9 shows two metrics derived from the 14 CB open operations recorded in November 2015 and January 2016 plotted against the sequence number of operations before the grading capacitor was replaced.

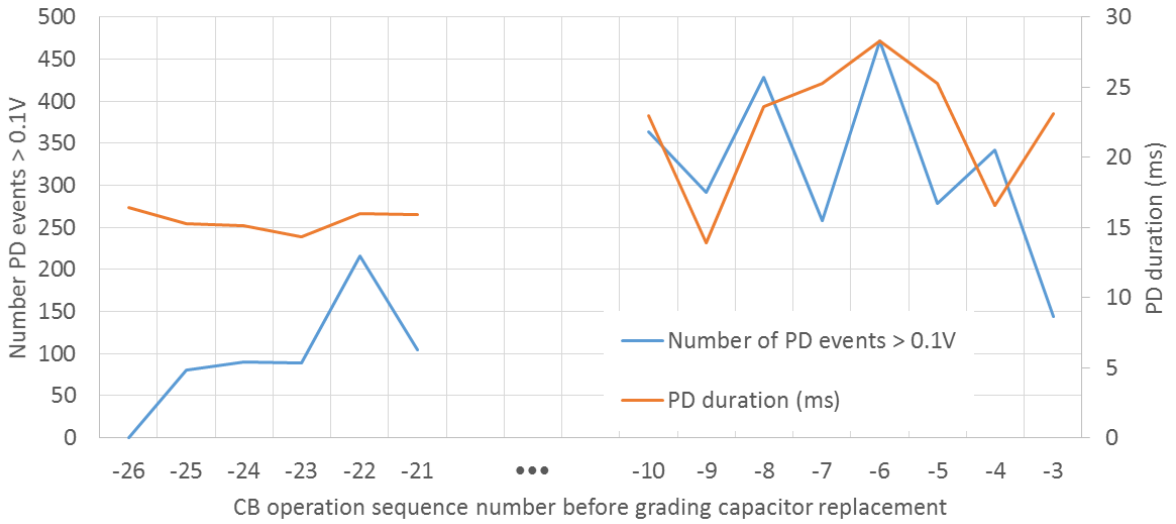

Figure 9 Grading capacitor PD versus CB operation sequence number

The metrics chosen can be simply derived from the measured data and were 1) the duration of the grading capacitor PD (i.e. the length of time in milliseconds over which PD impulses were emitted) and 2) the number of PD impulses which exceeded the 0.1V amplitude level. The latter metric was used to simply identify if the amplitude, as well as the duration of the PD impulses, was increasing. It can be seen from Figure 9 that there is a trend towards greater values of both metrics as the CB operation sequence progresses towards the grading capacitor end of life. In particular, during the very first measurement made in November 2015, all of the capacitor PD impulses were below 0.1V amplitude. Based on the recorded results, the first instance of the capacitor PD amplitude exceeding 0.1V indicates that the capacitor has ~25 operations before failure. This conclusion is, of course, based on a limited dataset involving one specific type of grading capacitor, however, it can inform the asset replacement process for utilities that have multiple instances of this type of capacitor. It is speculated that a similar analysis could derive suitable metrics for other types of grading capacitor exhibiting the same defect.

5. CONCLUSION

The methodology used to investigate the CB allows assessment of the grading capacitor PD and, additionally, the CB trip time, the breaker arcing time and the phase opening sequence. Results taken during the investigation were used as the basis for removing a grading capacitor from service and testing within an HV test laboratory. The grading capacitor identified showed extremely poor PD and dissipation factor results and was consequently stripped down, revealing that the capacitor was

effectively at end of life. Analysis of grading capacitor PD field measurements showed increased trends in both PD duration and intensity of emissions as the investigation progressed. The results demonstrate that the onset of PD activity exceeding 0.1 V - as measured using the foregoing methodology - occurred when the capacitor was within 25 operations of failure, although this conclusion is restricted to the specific type of capacitor and defect.

In relation to grading capacitors, the testing approach allowed the CB to remain in operational service which is a significant benefit compared to conventional on-site testing methods including tanδ and capacitance measurements which require an outage. Although equipment and sensors are deployed in proximity to the CB, the safety implications are moderate since no physical or electrical connection to the HV equipment is required, excepting current clamp connections in the marshalling kiosk. As described, the testing procedure required a set-up time of 2 hours and manual operation of the reactor CB via discussion with the Control Room. It is anticipated that further development of the testing procedure would allow the recording equipment to automatically trigger on scheduled operations of the CB without any Control Room intervention. Similarly, miniaturisation of the equipment would reduce the set up time. With both these improvements it should be economically feasible to screen all reactor CBs having grading capacitors on an annual basis. It is also anticipated that the method could be adapted for GIS reactive switchgear.

6. UPDATE DECEMBER 2020

This section describes the developments made since the paper was written in January 2020. A trial commenced in July 2020 to further develop the grading capacitor assessment technique and apply it to a range of AIS 400kV gas CBs from differing manufacturers. Note that the scope of the trial also includes assessment of the interrupters and the mechanism – it is hoped to report on this in due course. With respect to the grading capacitors, there are several differences between the equipment described in the previous sections and the equipment used in the trial:

- Previously, four antennas were used to identify emissions from individual grading capacitors. In the trial, only two antennas were used (to reduce the equipment count) which results in identification of a grading capacitor pair.
- The use of separate antennas and E-field sensors has been replaced with a combined device that performs both functions - again this reduces the equipment needed for the trial.
- Improved recording hardware now allows all relevant measurements to be automatically recorded following a trip coil current pulse, thus allowing the use of scheduled CB operations with no operator present. All data is retrieved remotely via a 3G modem.

The results are summarised in the table below which reports aggregate numbers of impulses in the following periods:

1. Between the trip pulse and the point of current interruption – ‘Before the interruption’ - the emissions in this period are related to the operation of the interrupters.
2. For a period of 100 ms following the point of current interruption – ‘After the interruption’ - during this period the grading capacitors are stressed to ~2 p.u. by the combination of the busbar voltage and the reactor transient, thus the impulses may be related to dielectric deterioration of the grading capacitors.

Date	Manu.	PD count	R	Y	B	Notes
Nov 2015	A	Before int.	36	25	21	Average of 4 trip ops
		After int.	308	0	0	

July 2020	B	Before int.	7	7	8	Average of 7 trip ops
		After int.	3	3	20	
Nov 2020	A	Before int.	14	17	16	Average of 3 trip ops
		After int.	0	0	0	

The first entry shows the original state of the CB described above (November 2015), which identifies a failing (red) grading capacitor. Note that the PD count after the interruption on the red phase could only be measured for 17 ms due to limitations in the recording device memory - the PD count would be considerably higher had the measurement continued for the full 100ms. In July 2020 a CB from a different manufacturer was assessed: it can be seen that some discharges occur following the interruption, but this figure is significantly higher on the blue phase. Since this may represent the incipient deterioration of the blue phase grading capacitor(s), this CB will now be monitored every year to establish a trend; it is not believed that any intervention is required at this stage. Finally, the original CB was re-assessed in November 2020 – nearly 5 years after the replacement of the interrupters and the grading capacitors: the results indicate that the CB is functioning correctly.

Appendix 1: Electric-field sensors used in the derivation of the reactor terminal voltages

The reactor terminal voltages were derived from measurements made with electric field sensors – see Figure A1.1 below. Each sensor consists of a Ø15 mm conductor held parallel to an earthed plate. Additional capacitors between the conductor and the earthed plate eliminated any 50 Hz phase shift.

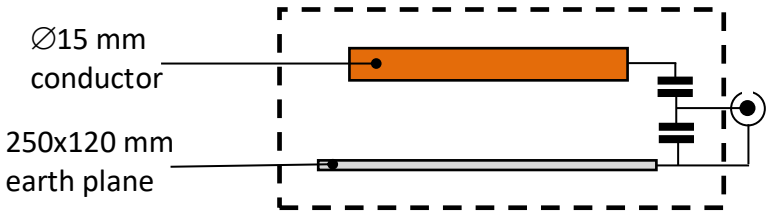

Figure A1.1 Outline of electric field sensor

Appendix 2: Average impulse emission count during the interrupter arcing period

Date	# ops recd.	Red phase		Yellow phase		Blue phase		Comments
		I	II	I	II	I	II	
5 Nov 2015	7	14	8	13	10	11	10	CB at ~2,600 operations
23 Jan 2016	8	7	2	8	5	8	8	After interrupter change
25 Feb 2016	4	4	5	5	4	2	2	After grading cap. change

I = interrupter nearest disconnector II = interrupter nearest reactor

Analysis of the PD emissions from the interrupters during the arcing period was anticipated to reveal useful information at the outset of the investigation when the synchronous opening relay was

suspected of incorrect operation, although all measurements from the CB indicated that the relay behaved correctly and no re-ignitions were detected. However, since the interrupters were replaced during the investigation, the results demonstrate the differences between PD emissions for new and mid-life interrupters. The table shows that the average impulse emission count is greatly increased when the CB had performed 2,600 operations. Since the interrupters were still serviceable at this point, the increased emission count is indicative of tolerable wear, rather than defect.

Appendix 3: Open operation for ideal CB (yellow and blue phases for Figure 6)

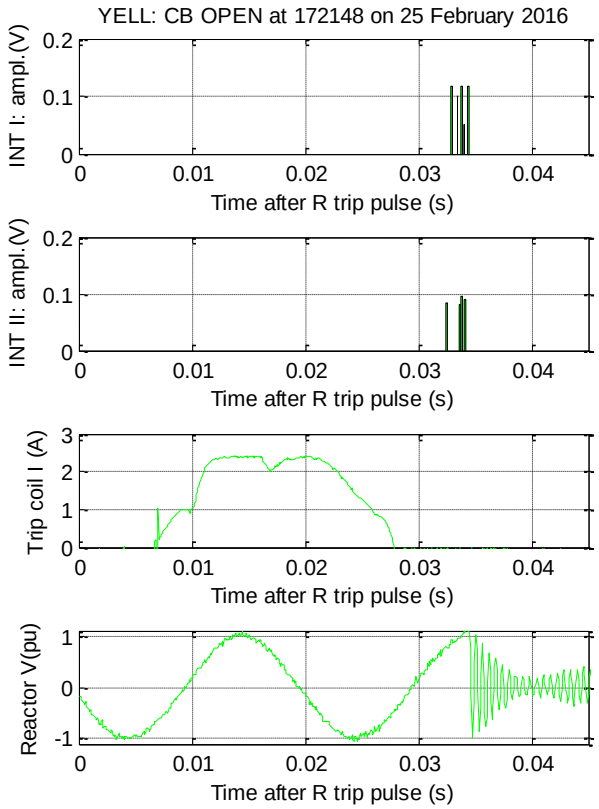

Figure A3.1 Yellow phase PD emission

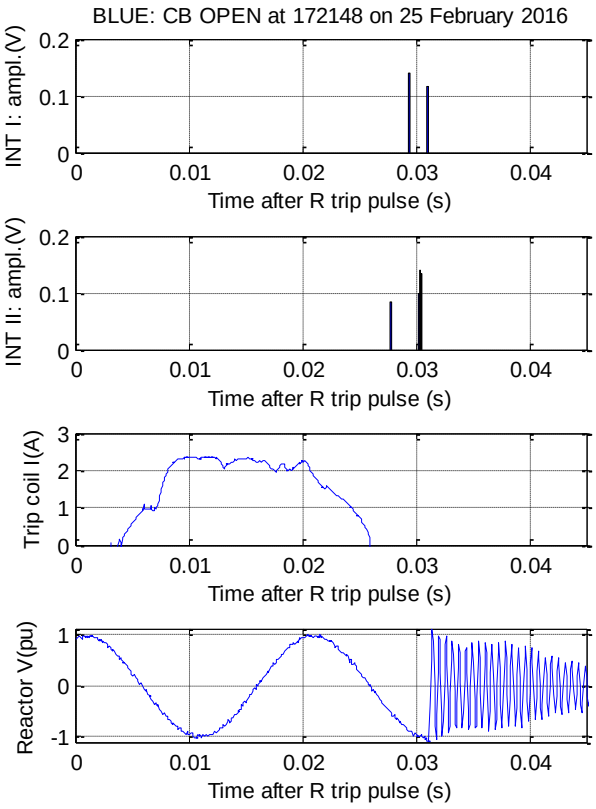

Figure A3.2 Blue phase PD emission

BIBLIOGRAPHY

[1] M Runde et al, 'Failures of voltage grading capacitors in GIS circuit breakers', (A3-306, CIGRE session, Paris, 2004).

[2] M Runde et al, 'Service experience with voltage grading capacitors', (A3-207, CIGRE session, Paris, 2006).

[3] Moore, P.J. et al, 'Radiometric Location of Partial Discharge Sources on Energised High-Voltage Plant', (IEEE Trans on PD, Vol 20, No 3, July 2005, pp 2264-2272).

[4] Portugues, I.E. et al, 'RF-Based Partial Discharge Early Warning System for Air-Insulated Substations', (IEEE Trans on PD, Vol 24, No 1, Jan 2009, pp 20-29).

[5] Moore, P.J., 'Radiometric measurement of Circuit-Breaker interpole switching times', (IEEE Trans on PD, Vol 19, No 3, July 2004, pp 987-992).

[6] Meier, S.D. et al, 'Radiometric Timing of High-Voltage Circuit-Breaker Opening Operations', (IEEE Trans on PD, Vol 26, No 3, July 2011, pp 1411-1417).